

Equation of state in the inner crust of neutron stars: discussion of the unbound neutron states

Jérôme Margueron, N. van Giai, N. Sandulescu

► **To cite this version:**

Jérôme Margueron, N. van Giai, N. Sandulescu. Equation of state in the inner crust of neutron stars: discussion of the unbound neutron states. International Symposium on Exotic States of Nuclear Matter, Jun 2007, Catania, Italy. in2p3-00184760

HAL Id: in2p3-00184760

<http://hal.in2p3.fr/in2p3-00184760>

Submitted on 1 Nov 2007

HAL is a multi-disciplinary open access archive for the deposit and dissemination of scientific research documents, whether they are published or not. The documents may come from teaching and research institutions in France or abroad, or from public or private research centers.

L'archive ouverte pluridisciplinaire **HAL**, est destinée au dépôt et à la diffusion de documents scientifiques de niveau recherche, publiés ou non, émanant des établissements d'enseignement et de recherche français ou étrangers, des laboratoires publics ou privés.

EQUATION OF STATE IN THE INNER CRUST OF NEUTRON STARS: DISCUSSION OF THE UNBOUND NEUTRONS STATES

J. MARGUERON and N. VAN GIAI

*Institut de Physique Nucléaire, Université Paris-Sud
F-91406 Orsay CEDEX, France*

N. SANDULESCU

*Institute of Physics and Nuclear Engineering,
R-76900 Bucharest, Romania*

In this paper, we calculate the stable Wigner-Seitz (W-S) cells in the inner crust of neutron stars and we discuss the nuclear shell effects. A distinction is done between the shell effects due to the bound states and those induced by the unbound states, which are shown to be spurious. We then estimate the effects of the spurious shells on the total energy and decompose it into a smooth and a residual part. We propose a correction to the Hartree-Fock binding energy in Wigner-Seitz cell (HF-WS).

Keywords: Equation of state, self-consistent mean-field model, pairing correlations.

1. Introduction

From the very first nuclear models based on extrapolations of a mass formula,¹ several models have been developed to provide the equation of state in the inner crust, like the BBP² and BPS³ semi-classical models or fully quantal self-consistent mean-field models.^{4-7,9,10} The latter models are based on the Wigner-Seitz (W-S) approximation and the continuum states are discretized in a box (spherical or not). In semi-classical models, a clear limitation is coming from the absence of nuclear shell effects which is known to play an important role in determining the composition of the ground state prior to the neutron drip,⁴ in the inner crust⁶ as well as in the transition zone between the crust and the core.¹¹ Since the seminal work of Negele & Vautherin,⁴ many efforts have been invested in the developpement of self-consistent mean-field modelization of the inner crust, by introducing deformation of the nuclear cluster in the high density part of the crust,^{5,10} or pairing correlations,⁷⁻⁹ or more recently by improving of the lattice description within the band theory.¹² Band theory takes into account the proper symmetries of the system, but the equations are numerically very complicated to solve and have not yet been solved in a self-consistent framework. Instead, it has been coupled to a self-consistent mean-field model at the W-S approximation.¹³ It has then been shown that the W-S approximation is justified if the temperature is larger than about

Table 1. Comparison of the proton number Z and the radius of the W-S cell R_{WS} obtained in different calculations. See the text for more explanations.

N_{zone}	k_F fm $^{-1}$	Z					R_{WS} (in fm)		
		N-V 4	HF-BCS a	HF	HFB	N-V 4	HF-BCS a	HF	HFB
2	1.12	40	20	22	22	19.6	15	16.6	16.6
3	0.84	50	36	22	20	27.6	24	20.6	20.6
4	0.64	50	56	24	24	33.2	36	26.2	26.6
5	0.55	50	58	28	20	35.8	40	30.4	27.0
6	0.48	50		28	20	39.4		32.0	29.2
7	0.36	40		22	20	42.4		36.0	33.4
8	0.30	40		22	22	44.4		38.2	37.8
9	0.26	40		22	22	46.4		38.0	38.8
10	0.23	40		36	36	49.4		46.6	47.0
11	0.20	40	52	36	28	53.8	57	48.4	43.8

Note: a The numbers shown in this column interpolate the results presented in Ref.⁹

100 keV, or if the quantity of interest averages the density of states on a typical scale of about 100 keV around the Fermi surface. The typical scale which has been found, 100 keV, is in fact related to the average inter-distance energy between the unbound states which are discretized in the W-S box. In this paper, we clarify the effect of the discretization of the unbound states on the ground state energy as well as the role of pairing correlations. Consequences for the equation of state are presented.

2. Equation of state in the inner crust

The inner crust matter is divided in 11 zones shown in Tab. 1, as in Ref.⁴ (notice that the denser zone has been removed since it is in the deformed pasta region). Each W-S cell is supposed to contain in its center a spherical neutron-rich nucleus surrounded by unbound neutrons and immersed in a relativistic electron gas uniformly distributed inside the cell. For a given baryonic density $\rho_B = A/V$, neutron number N and proton number Z , the total energy of a W-S cell, E_{tot} has contributions coming from the rest mass of the particles, $E_m(N, Z) = Z(m_p + m_e) + Nm_n$, from the nuclear components (including Coulomb interaction between protons) $E_n(\rho_B, N, Z)$, from the lattice energy,

$$E_l(\rho_B, N, Z, \{\rho_p\}) = \frac{1}{2} \int d^3r_1 d^3r_2 \rho_e(r_1) \frac{e^2}{|r_{12}|} (\rho_e(r_2) - \rho_p(r_2)) , \quad (1)$$

which is induced by the difference between the uniform electron density and proton density, and finally from the kinetic energy T_e of the relativistic electron gas.⁴ The Coulomb exchange energy as well as the screening correction for the electrons gas has been neglected.

The self-consistent Hartree-Fock-Bogoliubov (HFB) approach has been presented in detail in Ref.¹⁴ It has been extended to describe the dense part of the inner crust at finite temperature in Ref.¹⁵ With minor modifications, it has been

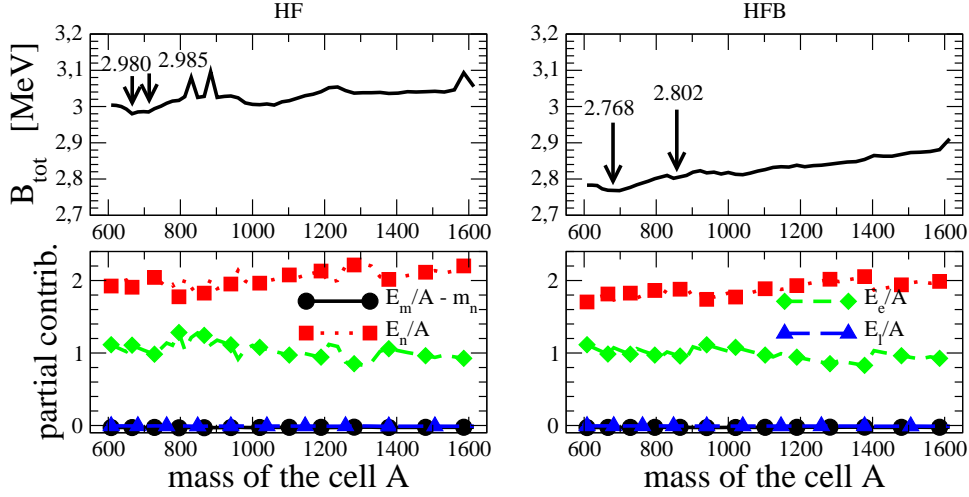


Fig. 1. The binding energy ϵ/ρ_B of the W-S cells in zone $N_{zone}=4$ as well as the partial contributions of the rest mass energy $E_m/A - m_n$, the nucleons, the electrons and the lattice. HF and HFB results are shown on the left and right panels, respectively. See the text for more details.

successfully applied to calculate the specific heat of the whole part of the inner crust.¹⁶ The effective N-N interaction should provide a reasonable description of both the nuclear clusters and the neutron gas. We use the Skyrme force SLy4¹⁷ which was adjusted to describe properly the mean field properties of neutron-rich nuclei and infinite neutron matter. The choice of the pairing force is more problematic since at present it is not yet clear what is the strength of pairing correlations in low density neutron matter. However, in the present paper we have chosen to adjust the effective pairing interaction on the results of the pairing gap obtained with the bare interaction. We then have a maximum gap in neutron matter of about 3 MeV located at $k_F = 0.85 \text{ fm}^{-1}$.

The minimization is performed in two steps: first, at a given density ρ_B and for a given mass number A , we look for the cell which satisfies the beta-stability criterion, $\mu_p + \mu_e = \mu_n$. The neutron and proton chemical potentials are provided by the HFB calculation while the electron chemical potential is deduced from $\mu_e = dE_{tot}/dN_e$. Note that, due to shell effects we may find several cells which satisfy this criterion. We then choose the one which has a minimal energy. In the second step, we minimize the total energy B_{tot} with respect to the mass number A . It should be noted that, in the second step all the cells must be calculated at the same density while the minimum energy is searched over the variable A . As the volume is modified by unit steps (the step of the mesh is 0.2 fm), the mass number A can take only discrete values so that $A = \rho_B V$ is always satisfied. The step between two values of A is not constant and vary as the square of the WS radius R_{WS} . We have approximatively $dA \sim \rho_B 4\pi R_{WS}^2 dR_{WS}$.

For $N_{zone}=4$, we show in Fig. 1 a typical example of step 2 in the search for the

W-S cell which minimizes the energy. On the l.h.s. is represented the total binding energy E_{tot}/A of the W-S cells obtained in Hartree-Fock (HF) mean-field model (without pairing). The position of the lowest minimum is indicated as well as two other local minima. In this case, there is a difference of 5 keV per nucleon between the two first minimum. On the r.h.s., we plot the results of HFB calculations which show the effects of the pairing correlations: the first minimum is deeper (about 34 keV per nucleons). On the lower part of the graph, we show the partial contributions of the rest mass energy $E_m/A - m_n$, the nuclear binding energy E_n/A , the electron kinetic energy T_e/A and lattice energy E_l/A . One sees that the inner crust is a typical example of frustrated system: when the nuclear energy is minimum, the electron energy is maximum and vice-versa. The minimum in energy is a compromise between these two opposite energies. The consequence is that it gives rise to numerous local minima which are not very far in energy from the absolute minimum.

The equation of state obtained at the HF and HFB approximations is given in Table 1. In total, 19714 cells configurations has been calculated. The pairing correlations do not strongly modify the HF results, it may slightly decrease the proton number and the WS radius. We also show previous calculations of equations of state. We have obtained proton numbers Z different from those of Refs.^{4,9} The results of Ref.⁴ have been obtained in a density matrix expansion framework interpolating microscopic calculations for homogeneous matter. The difference may be due to the fact that the Skyrme interaction SLy4 is based on more recent microscopic parametrizations. It is difficult to compare with the results of Ref.⁹ since those calculations have not been done at the same densities and they have essentially been carried out in the dense part of the crust. We then show an interpolation of their results. The comparison shows a similar trend in the dense cells.

3. Discussion of the shell effects

In ordinary nuclei, the bound states play an essential role in determining the ground state properties and the role of the continuum states is usually negligible. The coupling between bound states and continuum states can be more important for nuclei near the drip lines, as the Fermi energy is increasing. However, even in these most extreme situations continuum states are only virtually populated and the occupation numbers associated to continuum states are small compared to those of the bound states. In the inner crust of neutron stars, the situation is completely different: the Fermi energy is positive and most of the mass is due to the unbound neutrons while bound states account only for a small fraction. Thus, the continuum states contribute in an essential way to physical properties of the crust like its density, total energy or specific heat. The presence of bound states, or nuclear clusters, is not negligible but it induces only corrections to the ground-state properties.¹⁶ It is then very important to have an accurate model of the unbound states.

It should also be noted that, as the continuum states are embedded in a Coulomb

lattice, their asymptotic behavior is different from that occurring in nuclei. The continuum states are indeed periodically distorted within a distance equal to the lattice step (20-100 fm). The proper theory for the description of the continuum states is the band theory which requires to solve the Schrödinger equation,^{12,13} $(h_0 + h_{\mathbf{k}})u_{\alpha,\mathbf{k}}(\mathbf{r}) = \epsilon_{\alpha,\mathbf{k}}u_{\alpha,\mathbf{k}}(\mathbf{r})$, where h_0 is the usual single-particle Hamiltonian of mean-field models. The second term $h_{\mathbf{k}}$ is induced by the Floquet-Bloch boundary conditions for the single-particle wave function $\varphi_{\alpha,\mathbf{k}}$: $\varphi_{\alpha,\mathbf{k}}(\mathbf{r}) = u_{\alpha,\mathbf{k}}(\mathbf{r})e^{i\mathbf{k}\cdot\mathbf{r}}$. The spherical W-S approximation is obtained by setting $\mathbf{k} = 0$ and replacing the W-S elementary polyhedron by a sphere. Then, the remaining index α is discrete, like in usual mean-field models, and runs over the eigenstates of the Hamiltonian h_0 . The main difference between mean-field models and band theory is indeed due to the term $h_{\mathbf{k}}$. In band theory, this term introduces a new index \mathbf{k} which is a continuous variable ranging between 0 and π/a fm⁻¹ where a is the lattice step. As a consequence, the density of unbound states is continuous (notice that it may also have structures and gaps). It is then clear that the discrete distribution of unbound states present in usual mean-field models is a consequence of the dropping of $h_{\mathbf{k}}$ in the W-S approximation.

We can characterize the distribution of unbound states by the average distance between the unbound states energies, which can be related to the radius of the W-S cell as $\Delta\epsilon \sim \hbar/2mR_{WS}^2$: the smaller the W-S radius, the larger the average distance $\Delta\epsilon$. One could notice that the W-S radius is a function of the density and it is fixed by the equation of state, as shown in Table 1. At the W-S approximation, the distribution of unbound states is then also fixed by the density. The non-continuous distribution of unbound states could be interpreted as a spurious effect, induced by the W-S approximation, since in band theory calculations, the density of unbound states varies in a continuous way.¹³ One can then distinguish between the physical shell effects due to the bound states from the spurious shell effects due to the unbound states and the W-S approximation.

4. Spurious shell effects

In order to estimate the spurious shell effects due to the unbound neutrons, we simulate an homogeneous gas of neutron matter in W-S cell by removing all the proton states. In homogeneous matter, the energy density should be independent of the volume, then of the W-S radius, and it should depend only on the density. In our simulation of homogeneous matter, we then vary the W-S radius from 10 to 50 fm, at constant neutron density. We call $B_{WS-hom.}(\rho_{unb.}, R_{WS})$ the binding energy per particle obtained for a given W-S radius R_{WS} and for a given density of unbound neutrons $\rho_{unb.}$. We show the binding energy versus the W-S radius in Fig. 2(a) for several densities corresponding to $N_{zone}=6, 7$ and 8. It is clearly seen that the binding energy is not independent of the W-S radius, except for large W-S radii where the binding energy converge to the energy of homogeneous matter, $B_{hom.}(\rho_{unb.})$. The binding energy of homogeneous matter $B_{hom.}(\rho_{unb.})$ is calculated

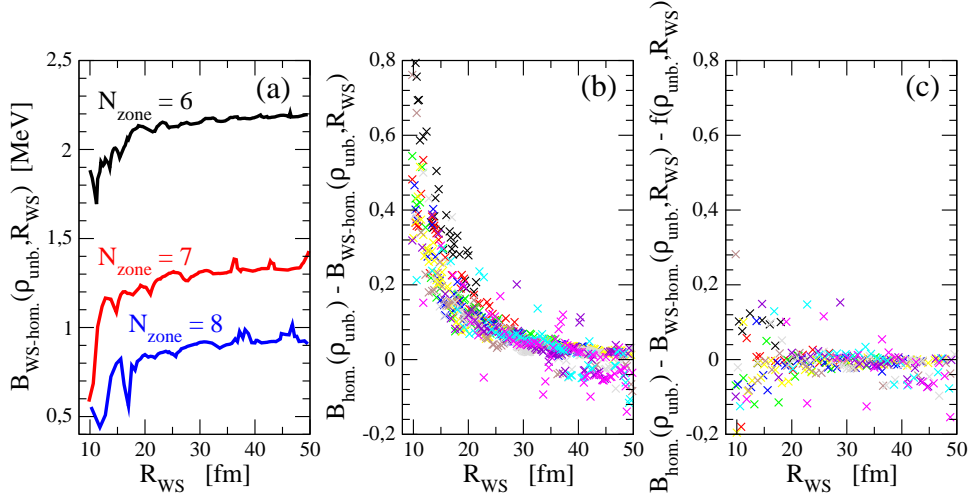


Fig. 2. We represent several quantities versus the W-S radius: (a) the binding energy $B_{WS-hom.}(\rho_{unb.}, R_{WS})$ corresponding to $N_{zone}=6, 7$ and 8 (b) the difference $B_{hom.}(\rho_{unb.}) - B_{WS-hom.}(\rho_{unb.}, R_{WS})$ (dots) and the function $f(\rho_{unb.}, R_{WS})$ which fit the smooth component (solid lines), and (c) the difference between the dots presented in (b) and the function $f(\rho_{unb.}, R_{WS})$.

from the average value of the Skyrme two-body interaction on a plane wave basis. The difference $B_{hom.}(\rho_{unb.}) - B_{WS-hom.}(\rho_{unb.}, R_{WS})$ is represented on Fig. 2(b) (dots). As expected, this quantity is converging to zero for large W-S radii, but for small radii, around 20 fm for instance, the difference can be as large as 300 keV per nucleons.

From the dots represented on Fig. 2(b), we obtain an universal function which fits the smooth radial dependence of the difference $B_{hom.}(\rho_{unb.}) - B_{WS-hom.}(\rho_{unb.}, R_{WS})$. As this effect is due to the discretization of the unbound states, it is proportional to the average distance $\Delta\epsilon$ between the box states. This difference should then decrease with the W-S radius as R_{WS}^{-2} . It should also be proportional to the number of unbound neutrons, while the density dependence is not known. We then represent it by a power law $\rho_{unb.}^\alpha$, where the power α is adjusted to reproduce the dots presented in Fig. 2(b). In this figure we show the fitted function,

$$f(\rho_{unb.}, R_{WS}) = 89.05(\rho_{unb.}/\rho_0)^{0.1425} R_{WS}^{-2}. \quad (2)$$

It interpolates the smooth part of the shell effects on the binding energy. There is, however, a residual difference which cannot be fitted. Finally, to estimate the residual difference between $B_{hom.}(\rho_{unb.}) - B_{WS-hom.}(\rho_{unb.}, R_{WS})$ and the adjusted function $f(\rho_{unb.}, R_{WS})$, shown on the r.h.s of Fig. 2(c). The average residual fluctuations are now of the order of 50 keV.

5. Modified HF binding energy in W-S cells (HF-WS)

In Sec. 4, it has been shown that the fluctuations in the binding energy induced by the spurious shell effect can be decomposed into a smooth and a residual term and we have obtained a universal function for the smooth term. We then propose a systematic correction to the HF binding energy in the W-S cell:

$$\begin{aligned} B_{HF-WS}(\rho_B, \rho_{unb.}, R_{WS}) &\equiv B_{WS-inhom.}(\rho_B, R_{WS}) \\ &\quad + \left(B_{hom.}(\rho_{unb.}) - B_{WS-hom.}(\rho_{unb.}, R_{WS}) \right)_{smooth} \\ &= B_{WS-inhom.}(\rho_B, R_{WS}) + f(\rho_{unb.}, R_{WS}). \end{aligned} \quad (3)$$

In the calculation of the total energy, the nuclear binding energy E_n/A should then be replaced by $B_{HF-WS}(\rho_B, \rho_{unb.}, R_{WS})$. The minimum energy can be unambiguously identified if the difference in energy between the first and the second minimum is larger than the residual fluctuation, about 50 keV. In the HF calculation, the difference in energy between different cell configurations are of the order of few keV to few tens of keV. The residual fluctuation of the proposed correction is then too large. However, as seen above, the pairing correlations help in producing a deeper first minimum. It may also help in reducing the size of the residual fluctuations. In a future investigation, we plan to obtain an improved binding energy for W-S cells including pairing correlations. It must be remarked that the effects of the coupling between the protons and the unbound neutrons have been neglected in B_{HF-WS} . This is a good approximation since the protons are deeply bound.

6. Conclusions

In the search for the W-S cells which minimize the energy, it is important to look not only at the lowest minimum energy, but also at the other minima. The differences between the first and other minima show how stable is the lowest minimum with respect, for instance, to thermal fluctuations or spurious shell effects. In HF calculations, the differences in total energy between the first minimum and the others are about few keV per nucleon (few MeV in total energy). It is shown that the spurious shell effects, induced by the W-S approximation, introduce a fluctuation in the calculation of the total energy up to about 300 keV per nucleon. Interpolating the smooth part of the spurious shell effects, we have then proposed a simple method to reduce the fluctuations down to about 50 keV per nucleon (HF-WS). The residual fluctuations are still too large, and the removal of the smooth part is not enough to improve the results obtained within the W-S approximation. We have also shown that the pairing correlations help in producing a deeper first minimum. We have then compared the equation of state obtained from HF and HFB binding energies. Several issues should still be addressed in future studies: spurious shell correction with pairing correlations as well as effects of the temperature. These two effects should give lower residual fluctuations than the one we obtained at the $T = 0$ HF approximation.

References

1. H. A. Bethe, G. Börner, and K. Sato, *Astron. and Astrophys.* **7**, 279 (1970).
2. G. A. Baym, H. A. Bethe, and C. J. Pethick, *Nucl. Phys.* **A175**, 225 (1971).
3. G. Baym, C. Pethick and P. Sutherland, *Astrophys. J.* **170**, 299 (1971).
4. J. W. Negele and D. Vautherin, *Nucl. Phys.* **A207**, 298 (1973).
5. P. Magierski, A. Bulgac, and P.-H. Heenen, *Nucl. Phys.* **A719**, 217 (2003).
6. F. Montani, C. May, H. Müther, *Phys.Rev.* **C 69**, 065801 (2004).
7. F. Barranco, R.A. Broglia, H. Esbensen, and E. Vigezzi, *Phys. Lett.* **B 390**, 13 (1997).
8. N. Sandulescu, N. Van Giai, and R.J. Liotta, *Phys. Rev.* **C 69**, 045802 (2004).
9. M. Baldo, E.E. Saperstein, and S.V. Tolokonnikov, *Nucl. Phys.* **A775**, 235 (2006).
10. P. Gögelein and H. Müther, arXiv:0704.1984.
11. A. Bulgac and P. Magierski, *Nucl.Phys.* **A683**, 695 (2001); *ibid.* **A703**, 892 (2002).
12. B. Carter, N. Chamel, and P. Haensel, *Nucl. Phys.* **A748**, 675 (2005).
13. N. Chamel, S. Naimi, E. Khan, and J. Margueron, *Phys. Rev. C* , 055806 (2007).
14. J. Dobaczewski, H. Flocard, and J. Treiner, *Nucl. Phys.* **A 422**, 103 (1984).
15. N. Sandulescu, *Phys Rev C* **70**, 025801 (2004).
16. C. Monrozeau, J. Margueron, and N. Sandulescu, *Phys. Rev. C* **75**, 065807 (2007);
C. Monrozeau, PhD thesis, Université Paris-Sud (2007), unpublished.
17. E. Chabanat. *et al.*, *Nucl. Phys.* **A627**, 710 (1997).